Petroleum and Coal

Article Open Access

ASSESSMENT OF SANDING POTENTIAL OF UNCONSOLIDATED SANDSTONE RESERVOIRS USING MODIFIED HOEK-BROWN FAILURE CRITERION

Fred Temitope Ogunkunle[1], S. O. Isehunwa[2], D. O. Orodu[1], Oluwasanmi Olabode[1]

[1] Department of Petroleum Engineering, Covenant University, Ota, Nigeria
[2] Department of Petroleum Engineering, University of Ibadan, Ibadan, Nigeria

Received May 10, 2018; Accepted July 27, 2018

Abstract

Assessment of sanding tendency during field development planning and completion design of oil and gas wells is very paramount because sanding tendency significantly impact on well completion choices and overall field development economics. Production of sand occurs in zones of failure creating perforation cavity and wellbore instabilities. The starting point of most predictive tool is identifying the stres-ses at the perforation cavity, failure prediction around such cavity and applying appropriate failure criterion. Most of the existing sand predictive tools are anchored on Mohr-Coulomb failure criterion which assumes a linear failure envelope but does not represent the response of reservoir rocks to induced stress.

Therefore, this work presents the results of a study investigating the potential of sand production in a Niger Delta field using modified Hoek-Brown failure criterion in developing a new geomechanical sanding predictive model that describes the non-linear increase in peak strength of isotropic rocks with increase in confining stress. The condition for sanding was formulated to be minimum well pressure at/below which sanding is to be expected. Based on Hoek-Brown material constant (a) which describes the rock mass quality, three (3) sanding criteria were developed and verified by comparing the results with existing numerical the model result and field scenario.

From the comparison with numerical model result, the three (3) sanding criteria gave the same result when Biot's constant is taken to be one (unity) but generally close to the numerical result. The results from the field case study, for the two wells evaluated indicates field well pressures that fall below the minimum well pressure at sanding predicted by the sanding criteria developed. This shows why they were both sand producers and this was in agreement with the production data from both wells. However, the model with exponent (a = 0.5) gave the closest to the field well pressure. The good agreement between the results from numerical/field case study and current work augurs well for its application when Hoek-Brown material constants can be accurately predicted.

Keywords: *Sand Production; Modified Hoek-Brown; Minimum well pressure; Wellbore Stability.*

1. Introduction

Every year, the upstream petroleum industry spends in excess of $6 billion US dollars on wellbore stability issues [10]. Many rock stability issues, some of which are sand production, borehole collapse otherwise called breakout, casing shear, rock compaction, and so on., are to be expected starting from the beginning of oil exploration operations such as; drilling and completion operations down to workover operations. Sand production is a usual production challenge observed in weakly consolidated and unconsolidated formation which play host to around 70 percent of global oil production [2].

Sand production arises when reservoir fluid flowing under high velocity removes a quota of the reservoir rocks creating continuous influx of formation materials. Production of sand occurs in zones of failure creating perforation cavity and wellbore instabilities. Sand production tendency over the life of the well has significant impact on completion choices. As we work in more challenging environments such as deep water, heavy oil, and high-pressure high-temperature wells, reservoirs are more complex and costlier to drill and complete. Downhole sand control methods significantly increase the complexity and cost of the completion and challenge the economics of the field development. This poses questions like do we need downhole sand control on all wells that have potential to produce sand? When the produced sand volume is not significant can the sand be managed at surface? Completions and workovers would be much simpler and cheaper without downhole sand control. Well production would also increase without downhole sand control, however, sand production could increase the risk of sanding up in wells [13]. It also increases the risk of eroding chokes, surface flow-lines, and equipment. Operational costs would increase due to sand transportation and disposal.

Numerous work has been done on the subject for so long, but despite that, accurately addressing this problem has remained unsolved because of its complexity. Several predictive tools are already been utilized in the industry to gain meaningful information about sanding potentials in oil and gas wells, most of which are limited in use because (1) they require information about the well that are not available until the well is completed and produced for a reasonable time frame, or not routinely measured on field [1,7], (2) some of the models are complex and requires extensive laboratory studies to determine the input data from core samples, which tend to affect the predictive accuracy [3,11], (3) inappropriate use of failure mechanism, (4) assuming a linear failure envelope for failure criterion which does not represent the response of reservoir rocks to induced stress (5) and finally considering intact rocks.

Chin and Ramos [4] developed a model for predicting sand production by coupling both geomechanical properties of rock and fluid flow parameters to estimate volumetric sand production in the early draw-down stage, bean-up, down to depletion stage. The work shows the influence of rock strength, flow properties, fluid properties and time on sand production from weak reservoirs. The model can serve as a guide to the quantity of sand to be expected. Mcphee and Enzendorfer [8] reported application of fuzzy logic computing techniques to correlate wireline log responses with core measurements to establish a field calibrated continuous sand production throughout the reservoir intervals. They used this method coupled with geomechanical models to analyse if selective perforation could guard well deliverability and equally ensure production without sand issues. The integrated sand management technique helped deliver production rate of over 100MMScf/d without sand production problems and also saved cost and lowering completion failure risk by using the fuzzy logic model to determine and avoid zones of thin sand which could lead to sand production. Isehunwa *et al.* [7] develop an analytical model to predict sand production in oil wells from the Niger/Delta oil fields, Nigeria. The model share input parameters close to Bratli *et al*. [2], with rock and fluid properties the major factor affecting sanding in their model. Their results show that maintaining cavity height below 30ft is important for sand free production.

In this paper, an analytical sand production onset prediction model is developed based on the popular theory of poro-elasticity and assuming shear failure induced sanding, the applicalibility of modified Hoek-Brown failure criterion rather than the popular Mohr-coulomb in predicting sand production onset was investigated.

2. Theoretical framework

The onset of sand production is the failure of intact rock, thus, if this can be predicted and prevented, then the sand production becomes no issue. Therefore, the starting point for most predictive tool for predicting sanding potentials in unconsolidated sandstones is identifying the stresses at the perforation cavity and failure prediction around the perforation cavity or open hole. The stepwise process in the model development is listed as follows:

1. Identifying the in situ stress magnitude.
2. Assessing the stress state at the borehole wall or perforation tunnel, having in mind the orientation of the borehole.
3. Applying appropriate failure criterion.

Assumptions

The approach in this model will be based on the listed assumptions:

- The horizontal stress is isotropic at far field
- The rock is a homogenous, unconsolidated or poorly consolidated sandstone
- The formation is in a geologically relaxed environmental, there is no active tectonic regime.
- Shear failure corresponds to initiation of sand production, i.e. no drag forces.
- Stress-controlled failure process around the perforation cavity is dominated by cohesion loss (i.e. not by frictional strength loss).
- The wellbore/perforation tunnel-formation structure is axisymmetric.
- Formation rock failure can be described by modified Hoek-Brown failure criterion.

2.1. Borehole stress (Isotropic In-situ stress)

The in-situ stresses in this study will be considered at points ($\sigma_{\theta=0}$). The three principal stresses can then be written in borehole geometry coordinates for conveniences and then transpose into radial systems of tangential, radial and overburden coordinates. For this study, the maximum induced stresses is taken to occur in the tangential coordinate. The borehole wall is assumed to be permeable, therefore, the pore pressure at the borehole wall is equal to the well pressure. The derivation of poro-elastic solution to stresses around the borehole according to Fjaer [5] given in terms of radial and tangential stresses are as follows,

$$\sigma_r{}' = (1-\alpha)P_{wf(t)} \tag{1}$$

$$\sigma_\theta{}' = \frac{P_{wf(t)}R_w{}^2 - \left(2\sigma_{h(t)} - P_{wf(t)}\right)R_e{}^2}{R_w{}^2 - R_e{}^2} - \alpha\frac{1-2\nu}{1-\nu}\bar{P}_{(t)} - \alpha\frac{\nu}{1-\nu}P_{wf(t)} \tag{2}$$

In this study, it is assumed that reservoir radius is in order magnitude greater the wellbore radius i.e., $R_e \gg R_w$, therefore, the above equation is simplified as follows;

$$\sigma_\theta{}' = 2\sigma_{h(t)} - \alpha\frac{1-2\nu}{1-\nu}\bar{P}_{(t)} - \left(1+\alpha\frac{\nu}{1-\nu}\right)P_{wf(t)} \tag{3}$$

2.2. Failure criteria

Several empirical criteria exist in the literature that describes the onset of rock failure, among these are the Mohr-Coulomb failure criterion; Mogi-Coulomb failure criterion; Ducker Prager failure criterion; Von Mises failure criterion and Hoek-Brown failure criterion which all give material behaviour of rocks at failure. The most common failure criterion used in theoretical modelling of sand production and any other geo-mechanical related problems is the Mohr-Coulomb failure criterion. It accounts for 80% of existing models while other criteria accounts for the remaining 20%, the major reasons for the use of Mohr-Coulomb failure criteria according to Oluyemi *et al.* [9] are (1) simplicity and ease of use (2) mathematical simplicity, which expressed shear stress as a linear function of normal stress. This thus implies a linear failure envelope and also only applicable when considering intact rocks. However, it has been proven that petroleum reservoir rocks do not exhibit linear failure envelope as such, modeling sand production while using Mohr-Coulomb or any modified version cannot be relied upon to fully capture failure behavior of rocks under imposed stress. Therefore, in this study, Hoek Brown failure criterion will be adopted, which is an empirically derived failure criterion that describes the non-linear increase in peak strength of isotropic rock with increasing confining stress.

The original non-linear Hoek Brown failure expression for intact was introduced in 1980 as;

$$\sigma_1 = \sigma_3 + \sqrt{mC_o\sigma_3 + sC_o{}^2} \tag{4}$$

where: $\sigma_1 = \text{major principal stress}$; $\sigma_3 = \text{minor principal stress}$;
$C_o = \text{uniaxial compressive strength of the intact rock}$; m and S are dimensionless empirical constants.

To account for reservoir rocks that are no longer intact, Hoek Brown criterion was updated in response to experience gained with its use and to address the practical limitation of friable rocks [6]. In achieving this, a generalized form of the criterion was reported in 1995 as follows;

$$\sigma_1{}' = \sigma_3{}' + C_o\left(m_b\frac{\sigma_3{}'}{C_o} + s\right)^a \quad (5)$$

m_b=is a reduced value of M in the original Hoek-Brown equation for failure,which accounts for the strength reducing effects of the rock mass conditions; a =empirical constant to account for system' s bias towards hard rock.

In terms of borehole stress,

$$\sigma_\theta{}' = \sigma_r{}' + C_o\left(m_b\frac{\sigma_r{}'}{C_o} + s\right)^a \quad (6)$$

$$m_b = m_i exp\left(\frac{GSI - 100}{24 - 14D}\right) \quad (7)$$

$$S = exp\left(\frac{GSI - 100}{9 - 3D}\right) \quad (8)$$

2.3. Critical Wellbore pressure failure model

If we assume isotropic in-situ stresses, and that the effective tangential stress is the maximum principal stress and the effective radial stress is the minimum principal stress, and if we assume sanding occur at shear failure condition, using Modified Hoek-Brown criterion, stability occur when RHS of equation 8 is equal the LHS as follows;

$$\sigma_r{}' = (1 - \alpha)P_{wf} \quad (9)$$

$$\sigma_\theta{}' = 2\sigma_{h(t)} - \alpha\frac{1 - 2\nu}{1 - \nu}\bar{P}_{(t)} - \left(1 + \alpha\frac{\nu}{1 - \nu}\right)P_{wf(t)} \quad (10)$$

$$2\sigma_h - \alpha\frac{1 - 2\nu}{1 - \nu}\bar{P} - \left(1 + \alpha\frac{\upsilon}{1 - \upsilon}\right)P_{wf} = (1 - \alpha)P_{wf} + C_o\left[m\frac{(1 - \alpha)P_{wf}}{C_o} + S\right]^a \quad (11)$$

To simplify equation 8 further, the Hoek-Brown material constants a, m_b and s for the rock mass has to be evaluated. These constants are determined for the rock mass using Geological Strength Index (GSI) as defined in Hoek *et al.* [6] (Table 1). Exponent "a" according to Hoek *et al.* was added to the failure criterion to address the system's bias towards hard rock and to better predict the behavior of poorer quality rock masses by enabling the failure envelope's curvature to be adjusted, especially under very low normal stresses. Since it is extremely difficult to estimate or predict the general state of reservoir rock downhole (rock quality) and especially when core examinations are not available. It will be inaccurate to assume reservoir rocks quality is 100% (hard rock, i.e a = 1) or that the rock mass is of very poor quality (a = 0). Therefore, for this research, two extreme scenarios and one average value of exponent "a" was used to simplify equation 8 further and hence, the derivation of critical well pressure that will give a safe margin was evaluated. The estimated values of the material constants (Table 1) are representation of the level of disturbance within the rock mass. The critical well pressures at different rock conditions are presented in table 2, derivations presented in appendix A.

3. Model verification

The validation process for models presented in Table 2 strictly relies on well log information (specifically sonic and density log). These data set are obtained during drilling process and provides specific data for the well before completion. In this case, the model can be used as a quick check for evaluating the potential for sanding across different reservoirs penetrated by a well, in terms of minimum allowable well pressure at/below which shear failure of the reservoir rocks will be triggered. With this, the completion team has a sanding predictive tool that can help in taking completion strategy decisions for well development. The sanding onset model presented in this study was verified using a field case study (Niger Delta) and data for numerical analysis from Yi [12].

Table 1. Hoek-Brown material constants for rock mass

Rocks	Carbonates Rocks	Shale	Sandstone	Fine Grained Igneous Rocks	Coarse Grained Igneous Rocks
Intact Rocks	M = 6 S =1	M = 8 S =1	M = 11 S =1	M =16 S =1	M = 18 S =1
Undisturbed Rocks	M = 3 S = 0.189	M = 4.39 S = 0.189	M = 5.59 S = 0.189	M = 7 S = 0.189	M = 12.56 S = 0.189
Moderately Weathered Rocks	M = 7 -1.6. S = 0.00198 – 0.0205	M = 1 -0.923. S =0.00198 – 0.0205	M = 1.6 - 3.02 S = 0.00198 – 0.0205	M = 1.6 - 4.81 S = 0.00198 – 0.0205	M = 3.3 - 6.51 S = 0.00198 – 0.0205
Heavily Weathered Rocks	M = 0.03 S = 0.00002	M = 0.043 S = 0.00002	M = 0.65 S = 0.00002	M = 0.0746 S = 0.00002	M = 0.109 S = 0.00002

Table 2. Conditions for sanding in wells with isotropic in-situ stresses and permeable borehole wall

Case	Material Constant (a)	Minimum bottom-hole pressures at failure
Isotropic In-situ Stress	$a = 0$	$P_{wfc} = \dfrac{2\sigma_h - \alpha n\bar{P} - C_o}{2 - \alpha n}$
Isotropic In-situ Stress	$a = 0.5$	$P_{wfc} = \dfrac{mC_oU - 2RY \pm \sqrt{mC_oU - 2RY^2 - 4R^2\left(Y^2 - SC_o{}^2\right)}}{2R^2}$
Isotropic In-situ Stress	$a = 1$	$P_{wfc} = \dfrac{2\sigma_h - \alpha n\bar{P} - SC_o}{2 - \alpha n + m(1-\alpha)}$
Yi [12]		$\dfrac{P_{wf}}{C_o} = (1-\nu)\left[2\dfrac{\sigma_h}{C_0} - \dfrac{1-2\nu\bar{P}}{1-\nu C_0} - 1\right]$

Case study 1 (Yi's numerical result)

The result from current study was compared with Yi's numerical prediction of minimum well pressure. The numerical results of Yi [12] were chosen because (Table 2), it shares similar boundary condition and physical geometry with the current work, except that the material failure criterion for the two models is different as discussed earlier in the introduction.

Using the data presented in Tables 3 and 4, critical wellbore pressure analysis was performed for the model and compared with Yi's numerical results. Based on the two models assumption, sand production is caused by wellbore shear failure, using the sanding models derived in this study and Yi's analytical model, together with his numerical results, the minimum well pressure for the three methods are presented in Table 4.

Table 3. Reservoir and production parameters from Yi [12]

Reservoir parameters	Value	Reservoir parameters	Value
Wellbore radius (ft)	0.25	X Direction permeability (mD)	5
Drainage area (acre)	40	Y Direction permeability (mD)	10
Aspection ratio	0.5	Z Direction permeability (mD)	0.1
Reservoir thickness (ft)	20	Porosity (fraction)	0.12
Gas specific gravity (fraction)	0.7	Reservoir temperature (°F)	108
Initial production rate (Mscf/Day)	1000	Formation compressibility (1/psi)	10e-6
Intial reservoir pressure (psi)	2800		

Table 3. Rock Mechanical properties used for comparison

Mechanical properties	Value	Mechanical properties	Value
Young Modulus (psi)	1.4E+6	Overburden Stress (psi)	3400
Poisson Ratio (fraction)	03	Min. Horizontal Stress (psi)	3060
Cohesive Strength UCS (psi)	1500	Poro-elastic constant	1
Friction Angle (Degree)	30		

Table 4. Comparison of current model with existing model and numerical result

This study			Numerical result
a = 0	a = 0.5	a = 1	Pw_f ((psi)
Pw_f ((psi)	Pw_f ((psi)	Pw_f ((psi)	
2114	2114	2114	2175

From Table 4, it can be seen that the onset of sand production for the three methods is not too different when Biot's constant ($\propto$) is taken to be 1 for all the models. The results are quite different for this current study when Biot's constant is not unity. Assuming Biot's constant to be 1 reduced the non-linear increase in peak strength of isotropic rock with increasing confining stress to a more general form of Mohr-coulomb linear failure envelope, which is the condition at which a = 0 in this current study. This understanding prompted us to carry out sensitivity study on the Biot's constant and its effect on the predicted minimum well pressure. The result of this is presented in Figure 1.

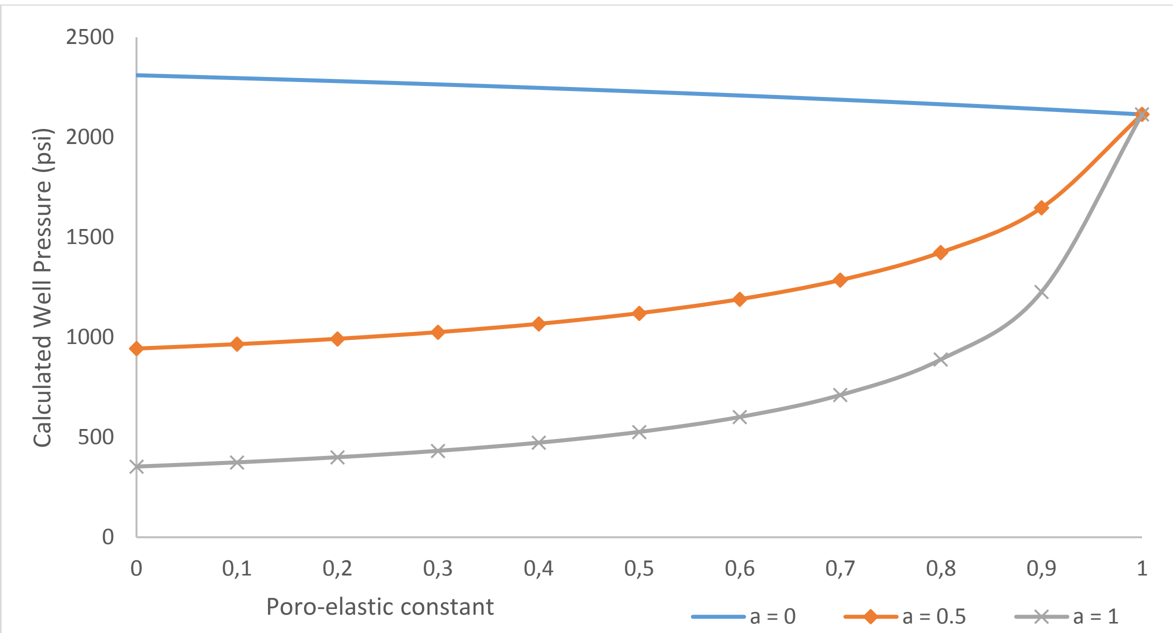

Figure 1. Effect of poro-elastic constants on calculated well pressure

In unconsolidated or weak formations, the Biot's constant α which is the ratio of bulk modulus at constant pore pressure to the bulk modulus at constant confining pressure is generally approximated to be 1. Figure 1 shows the effect of Biot's constant on the calculated well pressures. It can be observed from the Table 4 that, for the special case of ($\propto = 1$), the three conditions of rock mass quality according to table 2 gave the same minimum well pressure. This is due to the fact that Biot's constant was assumed to be 1, which eliminates the effect of other rock condition parameters according to Heok-Brown failure criterion for the cases of exponent "a" = 0.5 and 1. Sentivity study on Biot's constant between 1 and 0 shows two different trends for different conditions of exponent a; at a = 0, which is a typical case of linear failure envelope, reduction in poro-elastic constant resulted into increase in the calculated minimum pressure (Figure 1). Whereas at a = 0.5 and 1 shows similar trend of reduction in the calculated well pressure because the effect of Hoek-Brown material constants M and S which represent the frictional strength of the rock and measures of how fractured a rock is' respectively, are been accounted for. This implies that accurate estimation of Biot's constant is essential in accurately predicting the minimum well pressure below which sand is to be expected.

Case study 2 (Niger Delta)

Data from two exploration boreholes (well A and B) were used in this aspect. The strength of the reservoir rocks are direct results of compaction of the sand grains and effects of overburden and was found to be strongly correlated to depth as a function of burial. Tables 5 and 6 records the extracted sand production data for wells A and B, with the gas to liquid ratio. Proposed model for the current study presented in Table 2 was used to perform analysis of critical well pressure at onset of sanding on wells A and B. Table 7 through 10 present the in-situ stress data used in calculating the borehole stresses and the dynamic elastic properties used in the model.

Table 5. Sand production data for well A

Sand (PPTB)	Oil (bbl/m)	Water (bbl/m)	Water-cut (%)	Gas (Msc/m)	GLR (Scf/bbl)
2	54279	31	0	11063	204
0	21540	8	0	9525	442
1	13506	5814	30	5550	287
1	3646	1497	29	1024	199
2	39280	16440	30	7541	135
2	38743	7399	16	6933	150
2	23049	4228	15	4778	175

Table 6. Sand production data for well B

Sand (PPTB)	Oil (bbl/m)	Water (bbl/m)	Water-cut (%)	Gas (Mscf/m)	GLR (scf/bbl)
40	13081	36322	74	5919	120
34	17137	14032	45	82393	2643
33	15323	11686	43	2899	107
33	14850	10520	41	19075	752
33	19788	14790	43	14550	421
33	18150	13607	43	15624	492
33	18615	13327	42	5813	182

Table 7. In-situ stress data for well A

Depth(ft)	Overburden (Psi)	Pore Pressure (psi)	Min Horizontal Stress (psi)	Max Horizontal Stress (psi)
5842.9	4797.605	2752.006	3585.203	3877.348
5979.9	4975.875	2524.714	3765.543	4064.538
6059.9	5090.922	2580.002	3897.122	4200.117
6159.9	5179.737	2603.551	3981.947	4289.942
6259.9	5268.708	2626.481	4067.438	4380.433
6359.9	5357.834	2648.794	4153.595	4471.59
6459.9	5447.117	2670.49	4240.418	4563.413
6559.9	5536.556	2691.567	4327.908	4655.903
6659.9	5626.151	2712.027	4416.063	4749.058
6759.9	5715.902	2731.868	4504.884	4842.879
6859.9	5805.809	2751.093	4594.372	4937.367
6959.9	5895.872	2769.699	4684.526	5032.521
7059.9	5986.09	2787.688	4775.345	5128.34
7159.9	6076.465	2805.058	4866.831	5224.826
7200.9	6113.564	2812.002	4904.533	5264.578
7270.9	6260.245	2925.083	5267.767	5631.312
7344.9	6478.202	2917.982	5457.995	5825.24
7483.9	6750.478	2933.614	5583.738	5957.933
7574.9	7287.054	2794.987	6154.606	6533.351
7637.9	7492.78	2927.454	6424.238	6806.133

Table 8. Calculated dynamic elastic properties for well A (extracted for the reservoir)

Poisson ratio	Young modulus (Mpsi)	Shale Content (%)	Shear Modulus G (Mpsi)	Bulk Modulus K (Mpsi)	Biot's Constant
0.28	671.9335	0.113	262.4631	509.0334	0.46
0.28	687.6885	0.113	268.6171	520.9689	0.46
0.28	696.8885	0.113	272.2107	527.9385	0.46
0.28	708.3885	0.113	276.7027	536.6505	0.46
0.28	719.8885	0.113	281.1947	545.3625	0.46
0.28	731.3885	0.113	285.6867	554.0745	0.46
0.28	742.8885	0.113	290.1787	562.7865	0.46
0.28	754.3885	0.113	294.6707	571.4985	0.46
0.28	765.8885	0.113	299.1627	580.2105	0.46
0.28	777.3885	0.113	303.6547	588.9225	0.46
0.28	788.8885	0.113	651.1417	597.6345	0.46
0.28	800.3885	0.113	660.6337	1281.248	0.46
0.28	811.8885	0.113	670.1257	1299.657	0.29
0.28	823.3885	0.113	679.6177	1318.066	0.29
0.28	1749.819	0.3765	683.5094	1325.614	0.29
0.28	1766.829	0.3765	690.1538	1338.5	0.29
0.28	1784.811	0.3765	697.1779	1352.123	0.29
0.28	2334.977	0.221	912.1377	1768.895	0.2
0.28	2363.369	0.221	923.2288	1790.403	0.2
0.28	817.2553	0.1024	319.2642	619.1282	0.47

Table 9. In-situ stress data for well B

Depth(ft)	Overburden (Psi)	Pore Pressure (psi)	Min Horizontal Stress (psi)	Max Horizontal Stress (psi)
5694	4675.3	2448.4	4071.2	4355.9
5794	4675.3	2491.4	4205.6	4494.5
5894	4675.3	2534.4	4406.6	4701.3
5994	4675.3	2577.4	4581.8	4881.5
6094	4675.3	2620.4	4659.5	4986.8
6194	4675.3	2663.4	4786.7	5090.8
6280	4675.3	2700.4	4848.8	5162.8
6687	4675.3	2875.4	5283.4	5617.7
6931	4675.3	2911.0	5631.4	5978.0
7123	4675.3	2991.7	5991.2	6347.3
7809	4675.3	3201.7	6577.5	6968.0

Table 10. Calculated dynamic elastic properties for well B (extracted for the reservoir)

Poisson ratio	Young modulus (Mpsi)	Shale Content (%)	Shear Modulus G (Mpsi)	Bulk Modulus K (Mpsi)	Biot's Constant
0.28	654.81	0.113	255.7	495.9	0.46
0.28	666.31	0.113	260.2	504.7	0.46
0.28	905.8941	0.214	264.6	513.4	0.46
0.28	1456.542	0.214	568.8	1103.5	0.29
0.28	1480.842	0.214	578.3	1121.9	0.29
0.28	1505.142	0.214	587.8	1140.3	0.29
0.28	1526.04	0.214	765.5	1484.6	0.29
0.28	2086.344	0.532	815.1	1580.8	0.2
0.28	2162.472	0.221	289.7	562.1	0.2
0.28	762.161	0.221	297.7	577.7	0.47
0.28	835.563	0.221	326.4	633.3	0.47

Using three conditions for sanding (Table 2), the critical pressures at which sanding is to be expected were calculated and compared with field well pressure at sanding as shown in

Figure 2 and 3 for well A and B respectively. For well A, the condition for sanding as estimated from the sanding models developed gave the range of pressures for sanding to be between 1600 – 2200 psi using the 3 equations in this study, field data indicate that sand production occurs at well pressure of 2000 psi for perforated interval between 6843 ft to 6923 ft. From 2, a good match between field observed well pressure at sanding assuming shear failure and model predictions was observed which in turns induced sand production.

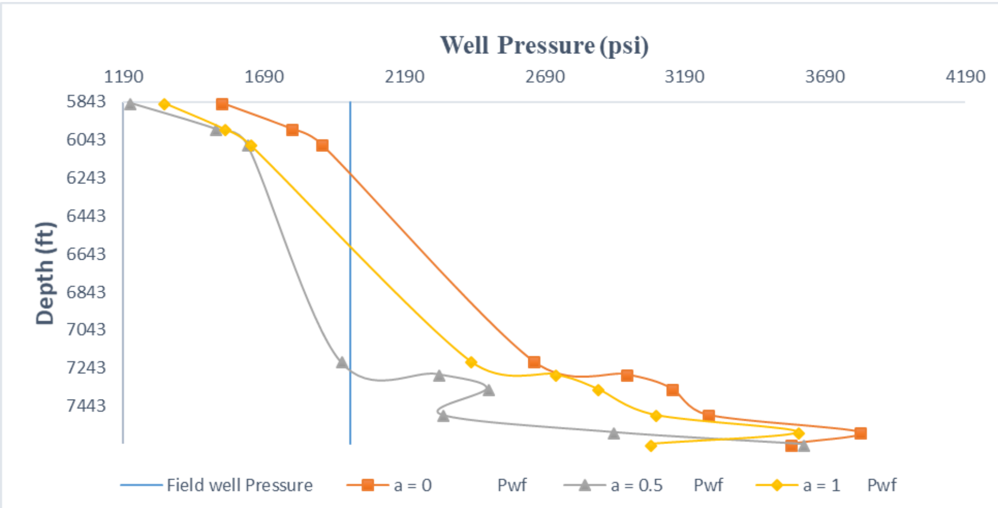

Figure 2. Plot of predicted and field measured well pressure at sanding onset assuming shear induced stress sanding for well A

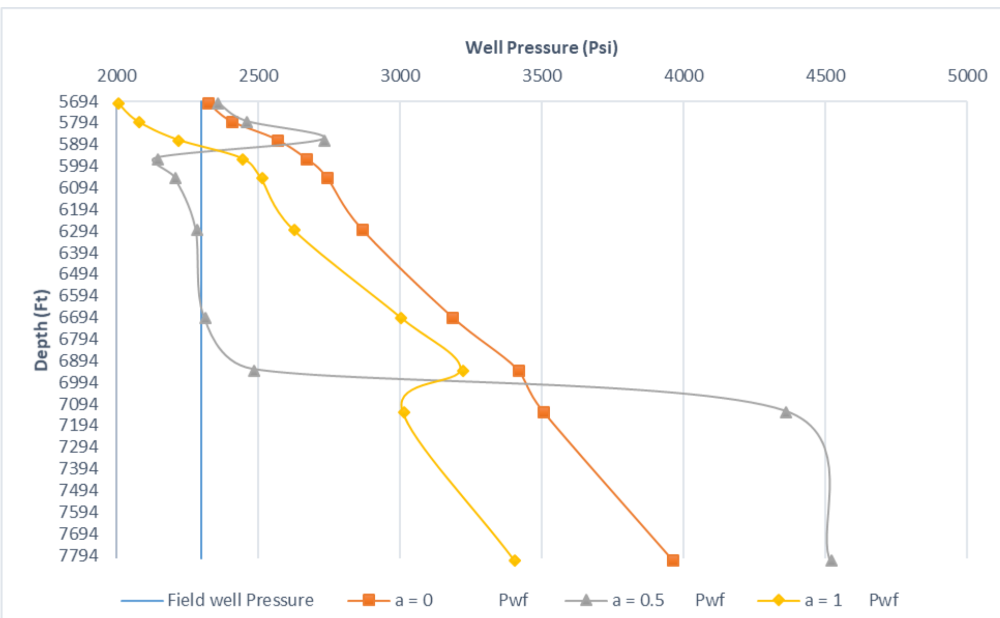

Figure 3. Plot of predicted and field measured well pressure at sanding onset assuming shear induced stress sanding for well B

For well B, sanding condition at a = 0.5 correspond to the field observed well pressure at sand production onset for perforation depth between 6294 ft to 6344 ft, while sanding onset at a = 0, 1 predicted slightly above the field observed minimum well pressure at sanding onset.

4. Conclusion

In this paper, the applicability of modified Hoek-Brown failure criterion in geomechanical modelling of sand production in unconsolidated sandstone reservoirs rock was explored and a new shear failure induced sanding onset prediction model is derived. The analytical model compared with the numerical result before been applied to field data to verify its field applicability. The results from the comparison were encouraging and very close. For field applications, the results were in agreement with field observed well pressure for the reservoirs penetrated. Therefore, this model is recommended for prediction of sanding potentials in unconsolidated sandstone reservoirs in real-time.

Nomenclature

$\sigma_r{}' = Effective\ Radial\ Stress$
$\sigma_\theta{}' = Effective\ Tangential\ Stress$
$\sigma_h = Minimum\ horizontal\ stress$
$\nu = Poisson's\ Ratio$
$\lambda = Lame\ Parameter$
$E = Young's\ Modulus\ (psi)$
$\alpha = Poro-elastic\ constant$
$\bar{P} = Far-field\ pore\ pressure\ or\ Average\ Reservoir\ Pressure\ (Psi)$
$P_{wf} = Bottom-hole\ Pressure\ (psi)$
$P_w = Well\ Presssure\ (Psi)$
$C_o = Uniaxial\ Compresive\ Strength$
$M = Hoek-Brown\ Material\ Constant\ (rock\ mass)$
$S = Hoek-Brown\ Material\ Constant$
$Re\ =\ reservoir\ boundary\ radius, L, ft$
$Rw\ =\ cavity\ (wellboe, perforation\ tunnel\ or\ perforation\ tip)\ radius, L, ft$

Appendix A

If we assume isotropic in-situ stresses, and that the effective tangential stress is the maximum principal stress and the effective radial stress is the minimum principal stress, and if we assume sanding occurs at shear failure condition, using Modified Heok-Brown criterion, stability occur when (eqn 8);

$$2\sigma_h - \alpha\frac{1-2\nu}{1-\nu}\bar{P} - \left(1+\alpha\frac{\upsilon}{1-\upsilon}\right)P_{wf} = (1-\alpha)P_{wf} + C_o\left[m\frac{(1-\alpha)P_{wf}}{C_o} + S\right]^a$$

ISOTROPIC IN-SITU STRESS

For $a = 0$ and solve for P_{wf}

$$2\sigma_h - \alpha\frac{1-2\nu}{1-\nu}\bar{P} - \left(1+\alpha\frac{\upsilon}{1-\upsilon}\right)P_{wf} = (1-\alpha)P_{wf} + C_o$$

$$2\sigma_h - \alpha\frac{1-2\nu}{1-\nu}\bar{P} - P_{wf}\left[1+\frac{\alpha\upsilon}{1-\upsilon}+1-\alpha\right] = C_o$$

$$P_{wf}\left[1+\frac{\alpha\upsilon}{1-\upsilon}+1-\alpha\right] = 2\sigma_h - \alpha\frac{1-2\nu}{1-\nu}\bar{P} - C_o$$

$$P_{wf} = \frac{2\sigma_h - \alpha\frac{1-2\nu}{1-\nu}\bar{P} - C_o}{\left[1+\frac{\alpha\upsilon}{1-\upsilon}+1-\alpha\right]}$$

Expanding the de-numerator yield;

$$\left[1+\frac{\alpha\upsilon}{1-\upsilon}+1-\alpha\right] = \frac{2(1-\upsilon)+\alpha(2\upsilon-1)}{1-\upsilon}$$

$$= 2+\alpha\left(\frac{2\upsilon-1}{1-\upsilon}\right)$$

$$= 2-\alpha\left(\frac{1-2\upsilon}{1-\upsilon}\right)$$

Let $n = \frac{1-2\upsilon}{1-\upsilon}$

Then the expansion above can be simplified as;
$2-\alpha n$
Therefore, $P_{wf}\ is$;

$$\boldsymbol{P_{wf}} = \frac{\boldsymbol{2\sigma_h - \alpha n\bar{P} - C_o}}{\boldsymbol{2-\alpha n}}$$

ISOTROPIC IN-SITU STRESS

For $a = {}^1/_2$ and solve for P_{wf}

$$2\sigma_h - \alpha\frac{1-2v}{1-v}\bar{P} - \left(1+\alpha\frac{v}{1-v}\right)P_{wf} = (1-\alpha)P_{wf} + \sqrt{mC_o(1-\alpha)P_{wf} + SC_o{}^2}$$

$$2\sigma_h - \alpha\frac{1-2v}{1-v}\bar{P} - \left(1+\alpha\frac{v}{1-v}\right)P_{wf} - (1-\alpha)P_{wf} = \sqrt{mC_o(1-\alpha)P_{wf} + SC_o{}^2}$$

Squaring both sides and re-arranging

$$\boldsymbol{P_{wf}}^2\left[\left(1+\frac{\propto v}{v}\right)^2 + 2\left(1+\frac{\propto v}{1-v}\right)(1-\propto) + (1-\propto)^2\right]$$
$$- \boldsymbol{P_{wf}}\left[4\sigma_h\left(1+\frac{\propto v}{1-v}\right) + 4\sigma_h(1-\alpha) - 2\propto\left(\frac{1-2v}{1-v}\right)\left(1+\frac{\propto v}{1-v}\right)\bar{P} - 2\propto\left(\frac{1-2v}{1-v}\right)(1-\propto)\bar{P} + mC_o(1-\propto)\right] + 4\sigma_h{}^2 - 4\sigma_h\alpha\frac{1-2v}{1-v}\bar{P} + \propto^2\left(\frac{1-2v}{1-v}\right)^2\bar{P}^2 - SC_o{}^2 = 0$$

Expanding the coefficients of $\boldsymbol{P_{wf}}^2$and $\boldsymbol{P_{wf}}$ yields the following

Coefficient of $\boldsymbol{P_{wf}}^2$

$$\left[\left(1+\frac{\propto v}{v}\right)^2 + 2\left(1+\frac{\propto v}{1-v}\right)(1-\propto) + (1-\propto)^2\right]$$

This can be written as;
$A^2 + 2AB + B^2$
Where

$A = \left(1+\frac{\propto v}{v}\right)$ $\qquad$ $A^2 = \left(1+\frac{\propto v}{v}\right)\left(1+\frac{\propto v}{v}\right)$

$B = (1-\propto)$ $\qquad$ $2AB = 2\left(1+\frac{\propto v}{1-v}\right)(1-\propto)$

$$A^2 = 1 + 2\frac{\propto v}{1-v} + \frac{\propto^2 v^2}{(1-v)^2}$$

$$AB = 1-\propto + \frac{\propto v}{1-v} - \frac{\propto^2 v}{1-v}$$

$$2AB = 2 - 2\propto + \frac{2\propto v}{1-v} - \frac{2\propto^2 v}{1-v}$$

$$B^2 = (1-\propto)^2 = 1 - 2\propto + \propto^2$$

Putting all these together gives;

$$1 + 2\frac{\propto v}{1-v} + \frac{\propto^2 v^2}{(1-v)^2} + 2 - 2\propto + \frac{2\propto v}{1-v} - \frac{2\propto^2 v}{1-v} + 1 - 2\propto + \propto^2$$
$$= \frac{4(1-v)^2 + \propto^2(2v-1)^2 + 4\propto(2v-1)(1-v)}{(1-v)^2}$$
$$= \frac{[2(1-v) + \propto(2v-1)]^2}{(1-v)^2}P_{wf}{}^2$$

Coefficient of $\boldsymbol{P_{wf}}$

$$P_{wf}\left[4\sigma_h\left(1+\frac{\propto v}{1-v}\right) + 4\sigma_h(1-\alpha) - 2\propto\left(\frac{1-2v}{1-v}\right)\left(1+\frac{\propto v}{1-v}\right)\bar{P} - 2\propto\left(\frac{1-2v}{1-v}\right)(1-\propto)\bar{P} + mC_o(1-\propto)\right]$$

Re-arranging this gives;

$$4\sigma_h\left[1+\frac{\propto v}{1-v} + 1-\propto\right] - 2\bar{P}\propto\left[\left(\frac{1-2v}{1-v}\right)\left(1+\frac{\propto v}{1-v}\right) + \left(\frac{1-2v}{1-v}\right)(1-\propto)\right] + mC_o(1-\propto)$$

Similar to $P_{wf}{}^2$ the coefficients of $\boldsymbol{P_{wf}}$ can be simplify thus;

$$A = \left[1 + \frac{\propto v}{1-v} + 1{-}\propto\right] = \frac{2(1-v){+}\propto(2v-1)}{1-v}$$

$$B = \left(\frac{1-2v}{1-v}\right)\left(1 + \frac{\propto v}{1-v}\right) + \left(\frac{1-2v}{1-v}\right)(1{-}\propto) = \left(\frac{1-2v}{1-v}\right)\left[1 + \frac{\propto v}{1-v} + 1{-}\propto\right]$$

$$= \frac{(1-2v)\left[\left(2(1-v)\right){+}\propto(2v-1)\right]}{(1-v)^2}$$

$$= 4\sigma_h A - 2\bar{P} \propto B + mC_o(1{-}\propto)$$

$$= 4\sigma_h\left[\frac{2(1-v){+}\propto(2v-1)}{1-v}\right] - 2\bar{P}\propto\left[\frac{(1-2v)\left[\left(2(1-v)\right){+}\propto(2v-1)\right]}{(1-v)^2}\right] + mC_o(1{-}\propto)$$

$$= \frac{2(1-v){+}\propto(2v-1)}{1-v}\left[\frac{4\sigma_h - 2\bar{P}\propto(1-2v)}{1-v}\right] + mC_o(1{-}\propto)$$

$$= P_{wf}\left[\frac{2(1-v){+}\propto(2v-1)}{1-v}\left[\frac{4\sigma_h - 2\bar{P}\propto(1-2v)}{1-v}\right] + mC_o(1{-}\propto)\right]$$

Constants

$$4\sigma_h{}^2 - 4\sigma_h\alpha\frac{1-2v}{1-v}\bar{P} + \propto^2\left(\frac{1-2v}{1-v}\right)^2\bar{P}^2 - SC_o{}^2$$

$$\boldsymbol{let\ n} = \frac{1-2v}{1-v}$$

The equation above can be written thus;

$$4\sigma_h{}^2 - 4\sigma_h\alpha n\bar{P} + \propto^2 n^2\bar{P}^2 - SC_o{}^2$$

To factor **n** into the expressions for P_{wf} and $P_{wf}{}^2$ the expressions can be written as;

Coefficient of P_{wf}

$$= \left[2{+}\propto\frac{(2v-1)}{1-v}\right]\left[4\sigma_h - 2\bar{P}\alpha\left(\frac{1-2v}{1-v}\right)\right] + mC_o(1{-}\propto)$$

$$[2{-}\propto n][4\sigma_h - 2n\bar{P}\alpha] + mC_o(1{-}\propto)P_{wf}$$

Coefficient of $P_{wf}{}^2$

$$= \left[\frac{2(1-v){+}\propto(2v-1)}{1-v}\right]\left[\frac{2(1-v){+}\propto(2v-1)}{1-v}\right]P_{wf}{}^2$$

$$= 2{-}\propto\left(\frac{1-2v}{1-v}\right)^2 P_{wf}{}^2$$

$$(2{-}\propto n)^2 P_{wf}{}^2$$

The final expression is as follows

$$(2{-}\propto n)^2 P_{wf}{}^2 - \left[[2{-}\propto n][4\sigma_h - 2n\bar{P}\alpha] + mC_o(1{-}\propto)\right]P_{wf} + 4\sigma_h{}^2 - 4\sigma_h\alpha n\bar{P} + \propto^2 n^2\bar{P}^2 - SC_o{}^2 = 0$$

To simplify the above expression further;

$$let\ k = (2{-}\propto n)^2$$

$$l = [2{-}\propto n][4\sigma_h - 2n\bar{P}\alpha] + mC_o(1{-}\propto)$$

$$w = 4\sigma_h{}^2 - 4\sigma_h\alpha n\bar{P} + \propto^2 n^2\bar{P}^2 - SC_o{}^2$$

Simplifying constant w, yields;

$$w = \propto^2 n^2\bar{P}^2 - 4\sigma_h\alpha n\bar{P} + 4\sigma_h{}^2 - SC_o{}^2$$

$$w = (\propto n\bar{P} - 2\sigma_h)^2 - SC_o{}^2$$

$$l = [2{-}\propto n][4\sigma_h - 2n\bar{P}\alpha] + mC_o(1{-}\propto)$$

$$= (2{-}\propto n) - 2[\propto n\bar{P} - 2\sigma_h] + mC_o(1{-}\propto)$$

Substituting the above simplifications back into the final equation gives;

$$(2{-}\propto n)^2 P_{wf}{}^2 - (2{-}\propto n) - 2[\propto n\bar{P} - 2\sigma_h] + mC_o(1{-}\propto)P_{wf} + (\propto n\bar{P} - 2\sigma_h)^2 - SC_o{}^2 = 0$$

Re-arranging this equation gives a quadratic equation that can be solve using general formula.

$$(2{-}\propto n)^2 P_{wf}{}^2 - P_{wf}[mC_o(1{-}\propto) - 2(2{-}\propto n)(\propto n\bar{P} - 2\sigma_h)] + (\propto n\bar{P} - 2\sigma_h)^2 - SC_o{}^2 = 0$$

$$x = \frac{b \pm \sqrt{b^2 - 4ac}}{2a}$$

$$a = (2{-}\propto n)^2$$

$b = [mC_o(1-\propto) - 2(2-\propto n)(\propto n\bar{P} - 2\sigma_h)]$
$c = (\propto n\bar{P} - 2\sigma_h)^2 - SC_o{}^2$
Let $R = 2-\propto n$ $Y = \propto n\bar{P} - 2\sigma_h$ $U = 1-\propto$
Then;
$a = R$ $b = mC_oU - 2RY$ $C = Y^2 - SC_o{}^2$
Therefore, P_{wf} is given as;

$$\boldsymbol{P_{wf} = \frac{mC_oU - 2RY \pm \sqrt{mC_oU - 2RY^2 - 4R^2\left(Y^2 - SC_o{}^2\right)}}{2R^2}}$$

ISOTROPIC IN-SITU STRESS

For $a = 1$ and solve for P_{wf}

$$2\sigma_h - \alpha\frac{1-2\nu}{1-\nu}\bar{P} - \left(1 + \alpha\frac{\upsilon}{1-\upsilon}\right)P_{wf} = (1-\alpha)P_{wf} + C_o\left[m\frac{(1-\alpha)P_{wf}}{C_o} + S\right]^a$$

$$2\sigma_h - \alpha\frac{1-2\nu}{1-\nu}\bar{P} - \left(1 + \alpha\frac{\upsilon}{1-\upsilon}\right)P_{wf} = (1-\alpha)P_{wf} + C_o\left[m\frac{(1-\alpha)P_{wf}}{C_o} + S\right]^1$$

$$2\sigma_h - \alpha\frac{1-2\nu}{1-\nu}\bar{P} - SC_o = P_{wf}\left[1 + \frac{\alpha\upsilon}{1-\upsilon} + 1 - \alpha + m(1-\alpha)\right]$$

$$P_{wf} = \frac{2\sigma_h - \alpha\frac{1-2\nu}{1-\nu}\bar{P} - SC_o}{\left[1 + \frac{\alpha\upsilon}{1-\upsilon} + 1 - \alpha + m(1-\alpha)\right]}$$

Let $n = \frac{1-2\upsilon}{1-\upsilon}$

Then the expansion above can be simplified as;

$$\boldsymbol{P_{wf} = \frac{2\sigma_h - \alpha n\bar{P} - SC_o}{2 - \alpha n + m(1-\alpha)}}$$

References

[1] Al-Awad MN and Desouky SEM. Prediction of Sand Production from a Saudi Sandstone Reservoir. Saudi Arabia: Revue de Institute français du petrole, 1997; 52(4): 407-414.

[2] Bianco LCB and Halleck PM Mechanisms of arch instability and sand production in two-phase saturated poorly consolidated sandstones. The SPE European Formation Damage Conference 2001. Hague, Netherlands: SPE-68932-MS, https://doi.org/10.2118/68932-MS.

[3] Bratli RK and Risne R. Stability and Failure of Sand Arches. Society of Petroleum Engineers Journals 1981, Pp. 236-248.

[4] Chin LY and Ramos GG. Predicting Volumetric sand Production in Weaak Reservoirs. SPE/ISRM Rock Mechanics Conference 2002. Trving, Texas: SPE/ISRM.

[5] Fjaer ERM. Holt,Horsud P, Raaen AR and Risnes R. Petroleum Related Rock Mechanics. Amsterdam, The Netherlands: Elsevier Science Publishers 1992.

[6] Hoek E, Carranza-Toress, CT & Corkum, B. Hoek-Brown failure criterion. 5th North American Rock Mechanics Symposium (NARMS-TAC) 2002. Pp. 00. 267 - 273). University of Toronto, Canada: Toronto Press.

[7] Isehunwa, SO, and Olanrewaju, O. A Simple Analytical Model for Predicting Sand Production in a Niger/Delta Oil Field. International Journal of Engineering, Science & Technology, 2010; 2(9): 4379 - 4387.

[8] Mcphee, CA and Enzendorfer CK. Sand Management Solutions for High Rate Gas Wells, Sawan Field Pakistan. *SPE International S*ymposium and Exhibition on Formation Damage Control 2004. Louisiana, USA: SPE.

[9] Oluyemi, GF & Oyeneyin, MB. Analytical critical drawdown (CDD) failure model for real time sanding potential prediction based on Hoek-Brown failure criterion. Journal of Petroleum and Gas Engineering, 2010; 1(2): 16 - 27.

[10] Powers, J. Halliburton and Geomechanics International Announce strategic partnership. Dallas, TX, USA: Press Release of Halliburton June 15, 2000.

[11] Weingarten, JS and Perkins TK. Prediction of Sand Production from Gas Wells: Methods and Gulf of Mexico Case Studies. Journal of Petroleum Technology, 1995; 596 -600.

[12] Yi X. Numerical and analytical modeling of sanding onset prediction. Texas: PhD Dissertation Submitted to the office of graduate Studies of Texas A & M University, 2003.
[13] Fadairo A, Oyedele-Adeyi O, Oladepo A, & Ogunkunle TF. Modeling the effect of entrained sand particles on pressure transverse in a flowing gas well. World Journal of Engineering, 2017; 14(5): 406-413.

To whom correspondence should be addressed: Frederick Temitope Ogunkunle, Department of Petroleum Engineering, Covenant University. Ota, Ogun State, Nigeria